frontiers in Earth Science

ORIGINAL RESEARCH
published: 13 November 2019
doi: 10.3389/feart.2019.00301

Effect of High Temperature and High Pressure of Water on Micro-Characteristic and Splitting Tensile Strength of Gritstone

Yu Zhao[1], *Jing Bi*[1,2]*, *Xiaoping Zhou*[2] *and Yansen Huang*[1]

[1] College of Civil Engineering, Guizhou University, Guiyang, China, [2] School of Civil Engineering, Chongqing University, Chongqing, China

To investigate the role of gritstone after hydro-thermal treatment on the mechanical properties and deformation failure behavior, the Brazilian test are carried out on gritstone specimens. Using load–displacement curves, the peak load and peak displacement of the gritstone specimens are analyzed in detail. The mechanical parameters are closely related to the high temperature, high pressure of water and the cooling down methods. The static splitting tensile strength (STS^S) of specimens are decreasing with the increase of water pressure. In the cooling down group, the STS^S and peak displacement of specimen WP1 are the lowest one. While, the STS^S of specimen W1 is the biggest one. The differences in mechanical properties of the gritstone specimen are mainly caused by the ablation effect in the microscale under different HTHP and cooling down conditions. The surface deformation characteristics of the tested gritstone specimens are investigated by analyzing the full strain field and the local strain concentration. In the gritstone specimen, the major principal strain is first concentrated in the bottom or the top of gritstone specimens where the crack is initiated. The small jump of local strain means crack initiation and propagation, while the fracture of strain gauge leads to strain mutation. The SEM results are discussed to describe the fracture mechanism of brittle gritstone after HTHP treatment.

Keywords: high temperature and high pressure, Brazilian test, the static splitting tensile strength, micro-characteristic, cooling down conditions

OPEN ACCESS

Edited by:
Hang Lin,
Central South University, China

Reviewed by:
Yanjian Lian,
Monash University, Australia
Yongkang Wu,
University of Massachusetts Amherst, United States

***Correspondence:**
Jing Bi
demonjjun@126.com

Specialty section:
This article was submitted to Earth and Planetary Materials, a section of the journal Frontiers in Earth Science

Received: *11 September 2019*
Accepted: *31 October 2019*
Published: *13 November 2019*

Citation:
Zhao Y, Bi J, Zhou X and Huang Y (2019) Effect of High Temperature and High Pressure of Water on Micro-Characteristic and Splitting Tensile Strength of Gritstone. Front. Earth Sci. 7:301. doi: 10.3389/feart.2019.00301

INTRODUCTION

Geothermal resources as a sustainable development of clean energy has promoted development of the world's ecological civilization construction such as structure adjustment and air pollution control. However, according to the principles of "heat extraction without water" and "irrigation with fixed production," the development of deep geothermal resources has been restricted by the difficulty of tail water recharge for a long time, especially the geothermal tail water recharge for sandstone thermal storage is a world problem. Therefore, it is necessary to understand the physical behavior of rocks under thermal action in order to improve the overall efficiency and flexibility of energy systems.

Thermal energy storage (TES) is an energy storage technology for solar energy, geothermal energy, industrial waste heat and other thermal energy resources. It commonly used in the heat mining of fractured geothermal reservoir and does not need to convert thermal resources into different forms of energy (Zhang et al., 2013; Pandey et al., 2014, 2018; Rawal and Ghassemi, 2014).

In Denmark, geothermal energy for district heating has been extracted from deep sandstone aquifers at temperatures as high as 75°C (Lund et al., 2011). Therefore, the possibility of storing excess heat seasonally in these geothermal aquifers was considered. The heat loss of these aquifers may be minimized due to the relatively high *in situ* temperatures and a low aquifer flow rates. In addition, heat storage can increase the thermal potential of aquifers and extend the service life of geothermal aquifers (Réveillère et al., 2013).

The temperature of the geothermal aquifers will be inevitably increased due to the heart storage. Temperature of water is known to play an important role to control both the extent and rate of reactions of minerals in the geothermal aquifer. In general, the reaction rates of mineral is increasing with the elevating temperature. While, the mineral solubility will be either increased or decreased when temperature is increasing, which is depending on the thermodynamic properties of the mineral (Griffioen and Appelo, 1993; Gruber et al., 2016). For instance, solubility of silicates increases with the increasing temperature. While, solubility of carbonates is much lower than that of silicates with the increasing temperature (Holmslykke et al., 2017). Dissolution/precipitation processes of rocks in the TES may affect the permeability of TES by changing the pore space geometry and pore connectivity of rocks (Ngwenya et al., 2000). Even further, dissolution of cementing material in rocks will probably reduce the mechanical strength of rocks in the TES. A major concern is therefore the hydro-thermal action may damage the structures of rocks making geothermal tail water recharge for sandstone thermal storage unfeasible.

Thermal energy storage systems in shallow aquifers injecting water with temperature about 20°C and small temperature differences ($\Delta T < 15°C$) are operating successfully in many countries (Réveillère et al., 2013; Bonte et al., 2014; Possemiers et al., 2014). Due to the limitation of test technique level, experiences with higher temperatures (about 150°C) is rarely reported (Vetter et al., 2012). However, field heat storage tests in closed shallow sandstone aquifers below 150°C show that calcium carbonate precipitation is the key hydrochemical problem (Holmslykke et al., 2017). Furthermore, researches on macro-mechanical strength of rocks in TES systems in shallow aquifers including traditional rock fracturing (Bi and Zhou, 2015, 2017a,b; Bi et al., 2016a,b; Zhao et al., 2016, 2017a,b, 2018a, 2019; Zhou et al., in press; Zhou and Bi, 2016), hydraulic fracturing (Breede et al., 2013; Zhao et al., 2018b), thermal fracturing (Zhou and Bi, 2018), shear stimulation (Zhu and Huang, 2019), and multilateral wells (Shi et al., 2018). And then, the mechanical characters of hot dry rock under thermo-hydro-mechanical (THM) effect (Breede et al., 2013; Possemiers et al., 2014; AbuAisha et al., 2016; Holmslykke et al., 2017; Schmidt et al., 2017; Chen et al., 2018; Kumari et al., 2018; Pandey et al., 2018; El Sharawy and Nabawy, 2019) also can be borrowed in to TES systems. These studies are focused on the influence of thermal effect on the mechanical properties of sandstone. While, the high temperature and pressure of water hydro-thermal influences on gritstone are few investigated, especially the coupled hydro-thermal effect on physical and mechanical properties of gritstone. However, in recent years, the behavior of rocks under thermos-mechanical coupling (TM) and measurement of basic physical and mechanical parameters is very complex (Hudson et al., 2009; Dutt et al., 2012; Bonte et al., 2014; Sengun, 2014; Singh et al., 2015; Shi et al., 2018; Wang and Konietzky, 2019). It includes rock deformation modulus, Poisson's ratio, tensile strength, compressive strength, cohesion, internal friction Angle, viscosity, thermal expansion coefficient and other changes with temperature (Gautam et al., 2016; Guha Roy and Singh, 2016; Yao et al., 2016; Sirdesai et al., 2017). Based on these researches, the high-temperature effects on the mechanical behaviors and physical characters of rocks are fully conducted. Although almost all the deep rocks exist in a hydrothermal environment, mechanical behavior of brittle rocks after the hydro-thermal treatment is few studied.

In order to discover the reason of reduction of the mechanical strength of rocks in TES, the primary purpose of this study is to investigate the effects of the high temperature and high pressure (HTHP) of water on the physical and mechanical properties of gritstone. The HTHP of water effect is to simulate the reservoir stimulation environment of TES. We conduct a series of laboratory experiments to investigate the breakdown pressure of high temperature gritstone specimens with different water pressure treatments. The vertical load and displacement of the treated specimens are monitored during the splitting experiments. The fracturing load-displacement curves, breakdown pressures, fracture patterns and evolution process of full strain field on the surface of the specimens after different treatments are compared. Finally, the physical characters including density of specimens are discussed in detail. The results obtained provide reference in the experimental basis, theoretical guidance and engineering safety for the reservoir stimulation of TES.

EXPERIMENTAL DETAILS

Specimen Preparation

In this study, the gritstone specimens are collected from interior formations in Jiangsu, China. The range of mineral particle size of the specimen is from 0.35 to 0.74 mm with an average size of 0.58 mm, which is the coarsest sandstone. Standard cylindrical gritstone specimens with the dimensions of 50 mm in diameter and 20 mm in length were prepared to evaluate the splitting strength. The prepared gritstone specimens have basic physical properties of the average density of 2.45 g/cm^3, the quasi-static compressive strength of 97.6 MPa and elasticity modulus of 135 GPa. There were six original specimens in total, which were divided into two groups with three specimens in each group. One group was marked as hydro-thermal treatment group (Ht group) and the other one group was marked as cool down group (Cd group), as shown in **Figure 1**.

Experimental Program

To represent the real environmental conditions of deep rock in TES, the heating schemes is executed that the hydro-thermal treatment with different water pressure. The specimens of Ht group are numbered and heated to the designed temperature

FIGURE 1 | Geometry of gritstone specimen and photos: **(A)** geometry; **(B)** the Ht group; **(C)** the Cd group.

of 150°C using an auxiliary heating device for 5 h under 10, 30, and 50 MPa, respectively. For the Cd group, specimens are also numbered and heated to the designed temperature of 150°C using an auxiliary heating device for 5 h under 50 MPa. Then, specimens are cooled down to room temperature using air, water and water with 50 MPa pressure in the autoclave as a quenching medium, respectively.

The heating rate of the device is set as in 0.5°C/min. For each test, the treated specimens were kept constant for 5 h once the temperature up to the target value (150°C) and pressure up to the target value (10, 30, and 50 MPa) in order to ensure the uniform heating of the specimens. The experimental result of specimens are marked as the 10M1, 30M1, and 50M1, which means that the pressure of the water is 10, 30, and 50 MPa, respectively. As for the hydro-thermal group, the specimens are heated to the designed temperature of 150°C by using a high-pressure autoclave for 10, 30, and 50 MPa, separately. The temperature of the high-pressure autoclave is kept in a range from 148°C ∼ 152°C. Corresponding to the cool down group, the specimens were maintained for 5 h under the target temperature state as the hydro-thermal group. The result was marked as the A1, W1, and WP1 in the cool down group, where A1 means that the specimens is cooled down to the normal temperature by exposing it to the air, but the temperature of specimens of W1 and WP1 are dropped down by putting into water and water quipped with 50 MPa pressure respectively. After the heating process, both the hydro-thermal and cool down treated specimens are cured under normal temperature condition (25°C) for more than 2 h. Then, the specimens are prepared for the next treatment. As shown in **Figure 2A**, the hydro-thermal environment of rock specimens is plotted. The treatment schedule applied on the sandstone specimens was depicted in **Figures 2B,C**. For recording the effects of gritstone after the hydro-thermal and cool down treatments, the mass of specimens is measured by an electronic balance after.

Testing Equipment

Figure 3 shows the HTHP autoclave and the servo-controlled materials testing machine RMT 301 used in this study, which are made by institute of rock and soil mechanics Chinese academy of science. The main equipment of HTHP autoclave includes temperature and pressure controller and HTHP cavity. The technical specifications of the HTHP autoclave are: the maximum temperature is 350°C, the maximum pressure of HTHP cavity is 65 MPa, and the heating rate of the device was controlled in 0.5°C/min. The main equipment includes a pressure device, a strut bar and support. The technical specifications of the RMT 301 are: the maximum loading is 1500 kN, the displacement control is 0.005–10 mm/min, the deformation control is 0.0001–1 m/s and can be applied to investigate the size effect of the specimen. The axial constant loading rate of this experiment was 0.02 mm/min until the specimen fails. During the splitting compression of gritstone specimens, the Digital Image Correlation (DIC) was also applied to record the evolution process of full strain feld on the surface of intact gritstone specimens.

TESTS RESULTS AND ANALYSIS

In accordance with the method recommended by Isrm (1978), the quasi-static split tensile tests, known as the Brazil test, are performed on gritstone specimens. During the loading process, the servo-controlled materials testing machine RMT 301 automatically records the vertical load and displacement of the loading point. As shown in **Figure 4**, the complete load-displacement curves of gritstone specimens under different water pressure and cooling down treating show a similar tendency, which are characteristics of four stages that the densification, elasticity, yielding and failure procedures (s is the displacement and F is the corresponding load). As for the load displacement curves of specimens after hydro-thermal treatments, the densification stage prolongs and the rate of slope decreases with the rise of water pressure. However, the yielding stage of treated specimens has no obvious difference compared to the original ones. For the load-displacement curves under two types of treatment conditions, the load quickly declines after it reached the peak load. It can be found from the comparison of the complete load-displacement curves of the original gritstone specimens with the result

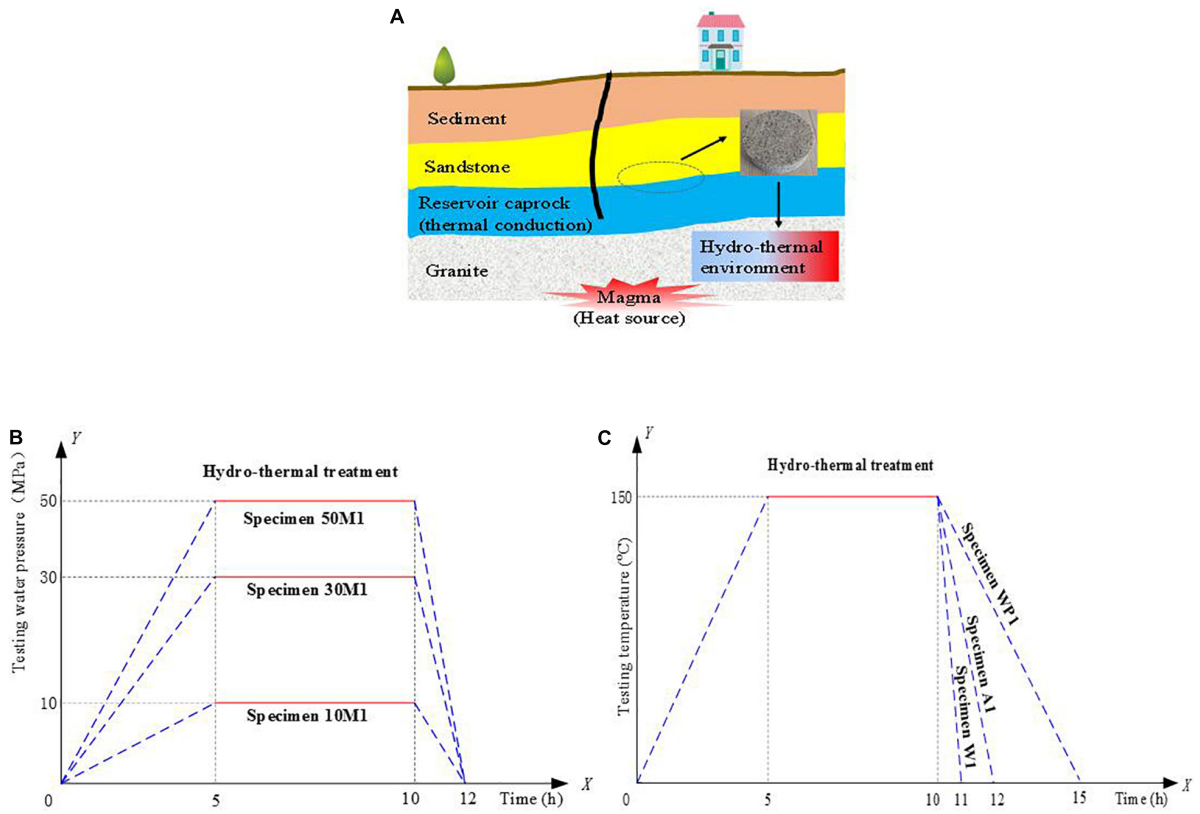

FIGURE 2 | Experimental background and project: **(A)** schematic diagram of deep rock environment; **(B)** schedule of hydro-thermal treatment; **(C)** schedule of cool down treatment.

of specimen with (cool or heat) treatment, it is likely that the brittleness has no difference between the two treated experimental conditions.

As seen in **Figure 4A**, for the gritstone specimens after hydro-thermal treatment, the curves move toward right because of the peak loads of specimens in Ht groups decrease with the obvious changing elasticity modulus when the water pressure bigger than 10 MPa. Furthermore, the densification stage of specimens extend with increasing water pressure. That is, the elasticity modulus decreases with increasing water pressure. Then, the peak loads decrease with increasing elasticity modulus. As shown in **Figure 4A**, the influence of hydro-thermal on specimens' strength and Young's modulus decreases with the increasing water pressure. While, when water pressure bigger than 30 MPa, the specimens' strength there is no obvious changes. That is to say, the hydro-thermal treatment has a greater influence on Young's modulus than that of strength of gritstone.

As seen from **Figure 4B**, the complete load-displacement curves of specimens in the Cd group are plotted, separately. In the Cd group, the peak load of specimens with same hydro-thermal and different cooling down treatments have obvious differences. For the specimen A1, which is cooled down in air, the densification stage is the longest one among the Cd group. Meanwhile, the Young's modulus of specimen A1 is bigger than that of specimen Wp1 but smaller than that of specimen A1 in the Cd group. For the specimen W1, which is cooled down in cool water, the densification stage and the Young's modulus have no obvious difference from the original specimen. While, the peak load of specimen W1 is bigger than that of original specimen. The reason will be discussed in the section "Discussion." For the specimen WP1, which is cooled down in water with 50 MPa pressure in the autoclave as a quenching medium, the Young's modulus is the smallest one in the Cd group. At the same time, the displacement and peak load are the smallest one in the Cd group. In author's opinion, it is may be caused by ablation of minerals in longer hydro-thermal action in the HTHP water condition. In order to discover the mechanism of ablation of minerals in hydro-thermal action of gritstone, the scanning electron microscope (SEM) technique is adopted to analyze the microscopic features of the splitting tensile fracture surface, and to study the micro-mechanism of hydro-thermal induced deterioration in the section "Discussion."

From the above, we can know that HTHP 150°C hydro-thermal treatment have an obvious effect on the densification stage, elasticity and failure procedures of gritstone. The densification stage prolongs and the rate of slope decreases with the rise of water pressure. Meanwhile, the strength and Young's modulus of specimens in Ht group decrease with increasing water pressure. While, the cooling down treatment has a great effect on the densification stage, elasticity and failure procedures of

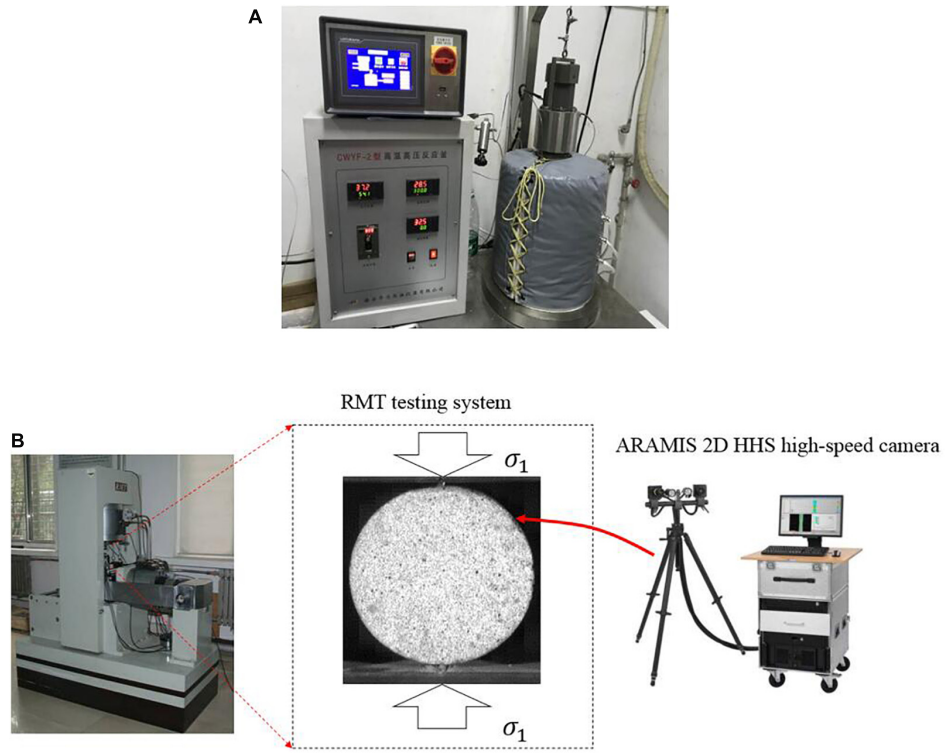

FIGURE 3 | Laboratory setup for: **(A)** the HTHP autoclave; **(B)** the schematic diagram of the compression split test.

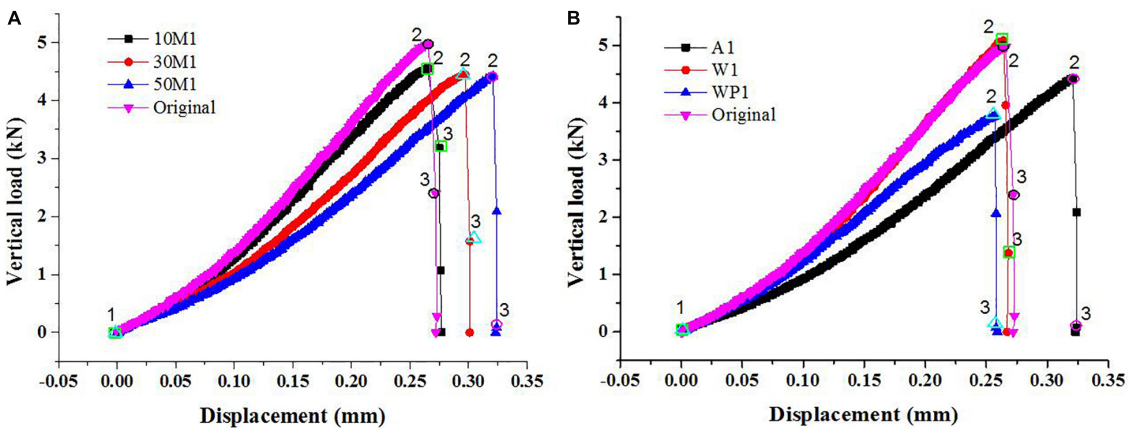

FIGURE 4 | Comparison of load-displacement curves of gritstone specimens under the two types of treatment conditions: **(A)** hydro-thermal treatment; **(B)** cool down treatment.

specimens in Cd group with no obvious pattern. The details will be discussed in the following subsection.

DISCUSSION

Strength and Failure Behavior of Treated Specimen

Table 1 represents the peak load (F_p), density (ρ), and peak displacement of the experimentally treated gritstone specimen, which is obtained from the load-displacement curves of **Figure 4**. Hydro-thermal and cooling down treatments have a significant impact on physical and mechanical properties of gritstone. The peak load of gritstone is positively correlated with the peak displacement, and the slope of the curve before the peak load decreases sharply with the increase of water pressure under the same temperature. In the Ht group, over the results of the entire treatment condition, the original F_p decreases from 4.966 to 4.422 kN of the specimen with water pressure of 50 MPa and water temperature of 150°C. In the Cd group, the curves of

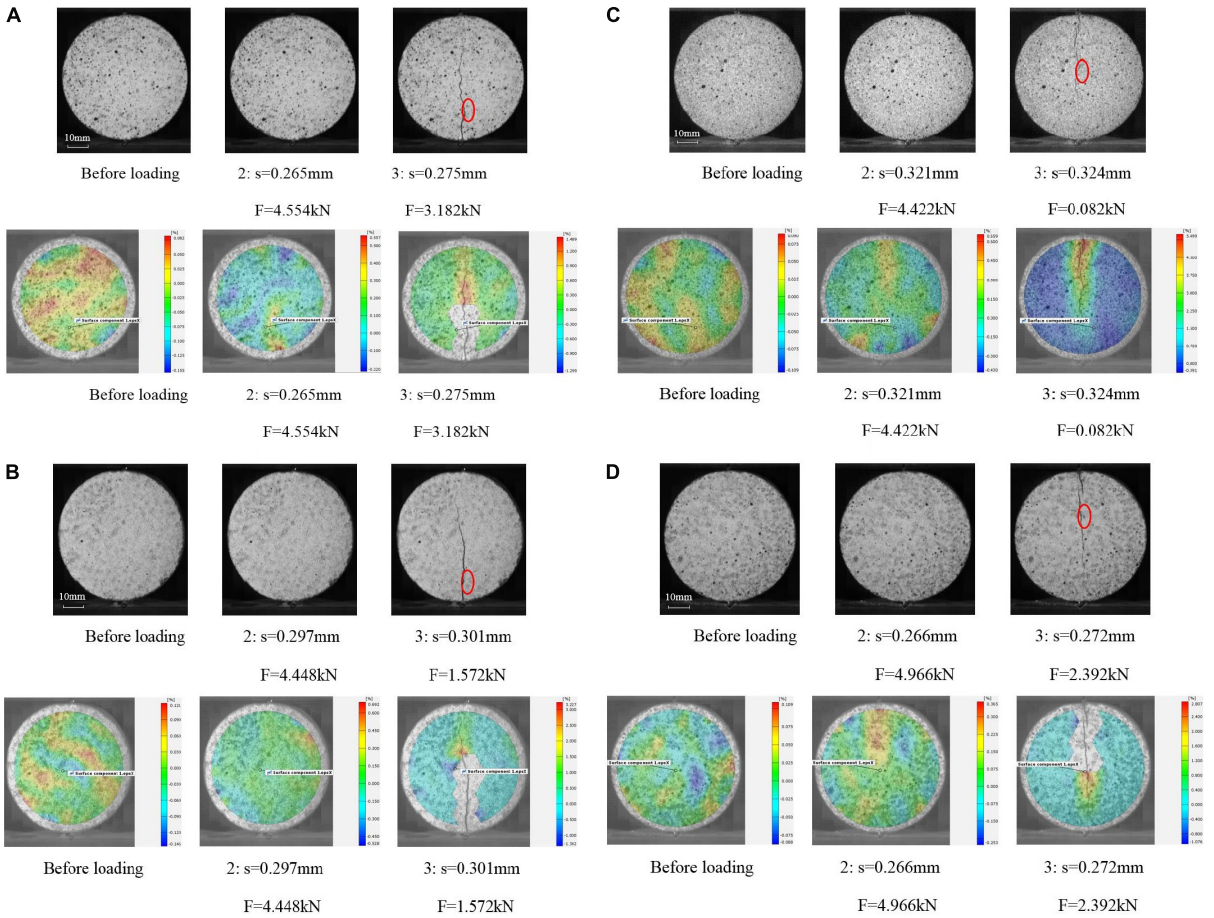

FIGURE 5 | Failure modes and evolution process of full strain field (Horizontal strain) on the surface of BD gritstone specimens in Ht group under static splitting tension (The Arabic numbers correspond to those in **Figure 4A**: **(A)** specimen 10M1; **(B)** specimen 30M1; **(C)** specimen 50M1; **(D)** original specimen. Red circle is the sampling position used in SEM.

load-displacement have no obvious pattern. The peak load of specimen W1, which is 5.082 kN, is the biggest one. When the specimen is cooled down in water with 50 MPa pressure in the autoclave as a quenching medium, the peak load is decreased to 3.764 kN. It is the smallest one in the Cd group. The static splitting tensile strength (STS^S) of gritstone is an important mechanical properties in the TES, and the STS^S of gritstone is determined following the given equation (Isrm, 1978):

$$STS^S = \frac{2F_P}{\pi dh}$$

where, $F_P$is the peak load of specimens fail, while, d and h are the diameter and thickness of the Brazilian disk specimens, respectively.

Digital Image Correlation is a non-invasive and non-destructive method for characterizing rock surface deformation. It has been applied to study the full strain fields of rock specimens under vertical loads (Yang et al., 2019). In this paper, speckle surface images of gritstone specimens after experimental treatments during the deformation process were obtained by the ARAMIS 2D HHS high-speed camera. The high-speed camera at a rate of up to 8,100 frames per second is used. By adopting an appropriate combination of frame rate and image resolution (896 × 896 Pixel@8,100 FPS), it is possible to document the cracking mechanisms precisely, in particular to determine whether shear or tensile crack occurs.

Then, the full strain field is calculated by using the GOM Correlate DIC analysis software to analyze the surface deformation characteristics of BD (The Brazilian disk) gritstone specimens under static splitting tension experiment. **Figures 5**, **6** show the typical fracture pattern of specimens after different treated conditions under static splitting tension experiment. From **Figures 5**, **6**, we can see that with an increase of water pressure, the failure mode of gritstone are same and failure. The major principal strain is first concentrated in the bottom or the top of gritstone specimens where the crack is initiated. Because that the static splitting tensile experiment in this paper of BD gritstone specimens is using point loading based on ISRM (Ulusay, 2014) suggested method. This pattern fits well with other researches (Bahaaddini et al., 2019).

The STS^S, density (ρ), and peak displacement of treated gritstone specimens are listed in **Table 1**. In the Ht group, the

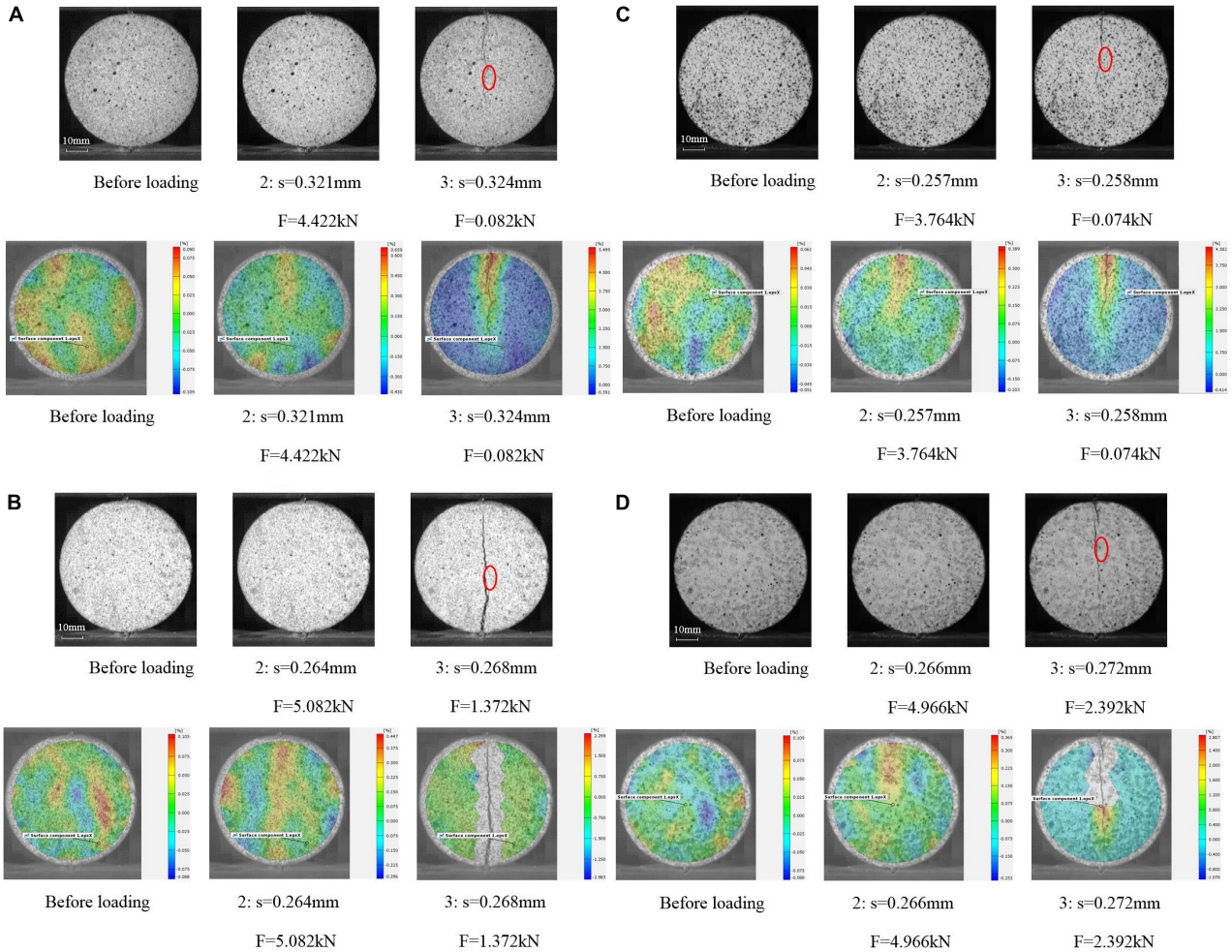

FIGURE 6 | Failure modes and evolution process of full strain field on the surface of BD gritstone specimens in Cd group under static splitting tension (The Arabic numbers correspond to those in **Figure 4B**): **(A)** specimen A1; **(B)** specimen W1; **(C)** specimen Wp1; **(D)** original specimen. Red circle is the sampling position used in SEM.

TABLE 1 | The static splitting tensile strength (STS^S), density (ρ), and peak displacement of treated gritstone specimens after the experimentally.

Specimen	Experimental treatment	STS^S (MPa)	Density (kg/m^3)	Peak displacement (mm)
BD specimens in HT group	Temperature/Pressure	–	–	–
Original	25°C/0 MPa	3.161	2.885	0.266
10M1	150°C/10 MPa	2.899	2.893	0.265
30M1	150°C/30 MPa	2.832	2.915	0.297
50M1	150°C/50 MPa	2.815	2.908	0.321
BD specimens in HT group	Cool down treatment	–	–	–
Original	–	3.161	2.885	0.266
A1	Cool down in air	2.815	2.908	0.321
W1	Cool down in water	3.235	2.928	0.264
Wp1	Cool down in water with 50 MPa pressure	2.396	2.969	0.257

STS^S of specimens are decreasing with the increase of water pressure. The STS^S decreases from 2.899 MPa of specimen 10M1 to 2.815 MPa of specimen 50M1. Meantime, the peak displacement is increasing with the increase of water pressure. In the Cd group, the STS^S and peak displacement of specimen Wp1, which is 2.396 MPa and 0.257 mm, respectively, are all the lowest one among Cd group. While, the STS^S of specimen W1, 3.235 MPa, is the biggest one. In the authors' opinion, the

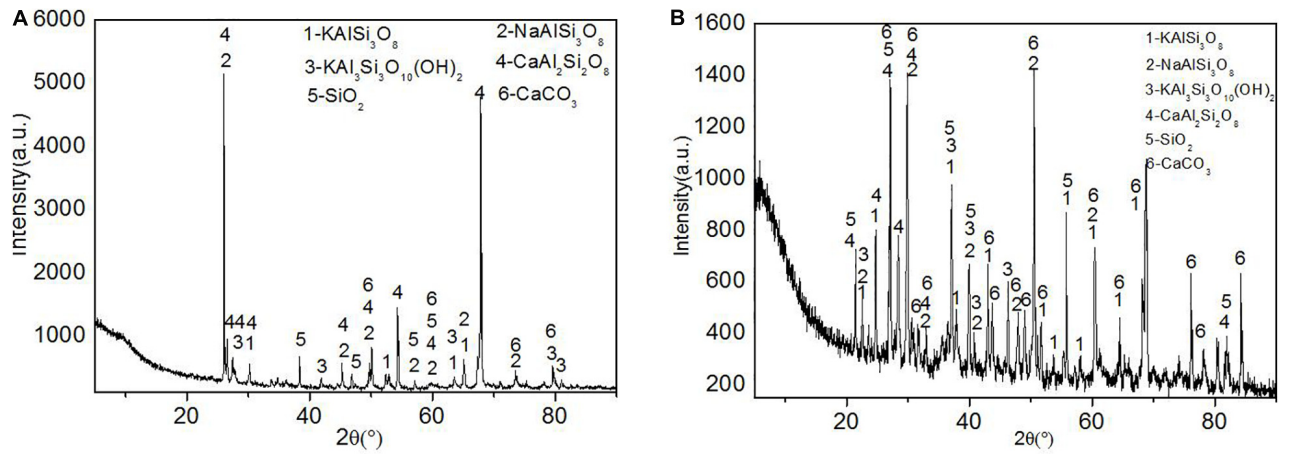

FIGURE 7 | X-ray diffraction of specimen with different treatment conditions: **(A)** original specimen, **(B)** specimen 50M1.

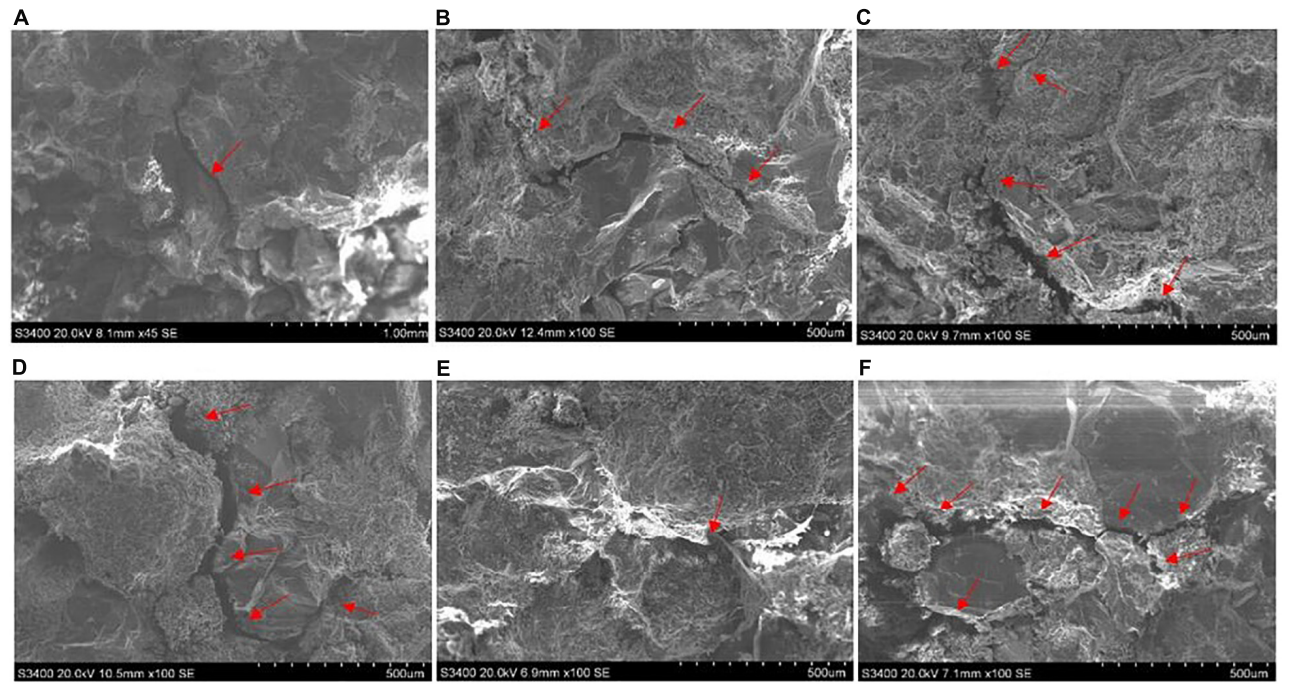

FIGURE 8 | Representative SEM images of gritstone after different HTHP treatments: **(A)** original specimen; **(B)** specimen 10M1; **(C)** specimen 30M1; **(D)** specimen 50M1; **(E)** specimen W1; **(F)** specimen WP1. Red arrow indicates the micro-crack.

differences in mechanical properties of the gritstone specimen are mainly caused by the ablation effect in the microscale under different HTHP and cooling down conditions. In order to further reveal its principle, the SEM results will be discussed detail in the following subsections.

Morphological Analyzation

All the experimental treatments cause the internal structure to change remarkably, such as fissure expansion, dehydration and the enlargement of voids. For sandstone under hydro-thermal treatments, the hydro-thermal influence on specimens can be simply considered as the confining pressure in local and lead to local damages. In order to discover the fracture mechanism of sandstone after hydro-thermal treatments on the micro levels, the X-ray diffraction experiments are conducted and the results are presented in **Figure 7**. It can be seen from **Figure 7** that the primary minerals of sandstone are $KAlSi_3O_3$, $NaAlSi_3O_3$, $KAlSi_3O_{10}(OH)_2$, $CaAl_2Si_2O_3$, SiO_2, and $CaCO_3$. For the original specimen, the content of $CaAl_2Si_2O_3$ and $NaAlSi_3O_3$ are higher than those of other mineral components. Under the action of the hydro-thermal treatment, mineral composition began to decompose and mineral content decreased.

For specimen 50M1, it has a hydrothermal ablation effect on mineral components, which results in a greater reduction of mineral components of $CaAl_2Si_2O_3$ and $NaAlSi_3O_3$. So, the effect of hydro-thermal treatment on mineral composition content is obvious. It is an important factor affecting on gritstone strength.

Figure 8 shows the microscopic observations of BD gritstone specimens after different HTHP treatments based on SEM. SEM mainly uses secondary electron signal imaging to observe the surface morphology of specimens. For the SEM specimen preparation, the first step is determining sampling site from large specimen. Secondary, the surface block of the sample is obtained by cutting method. Then, treatments of cleanout, burnish, etching, and gold spraying on the surface block is needed. It should be noted that the microstructure images are obtained from the sections of specimens that are treated by different HTHP treatments (Yang et al., 2019). In order to obtain the best results, three thin sections are made under each condition for SEM. Under the same conditions, the micro-observations of different sections are very close. Therefore, **Figure 8** presents the representative results, which are selected from the three sections for each HTHP condition. Furthermore, the difference in number and morphology of cracks in specimens due to the different treatments can generically represent the hydro-thermal effect on the microstructure of gritstone. The micro-crack of original specimen is observed at room temperature without any experimental treatment (**Figure 8A**). When the temperature and water pressure increase to 150°C and 10 MPa, respectively, the crack grows longer and wider (**Figure 8B**). When the temperature is keeping 150°C, and the water pressure increasing to 30 and 50 MPa, relatively hydro-thermal crack keeps growing longer and wider than that of specimens under water pressure of 10 MPa (**Figures 8C,D**). In the cooling down group, due to the effect of low-temperature water, the width and length of crack decreases (**Figure 8E**). When the specimen WP1 is cooled down in water with 50 MPa pressure in the autoclave, the width, length, and number of cracks increase sharply comparing to other specimens in Cd group.

Based on the X-ray diffraction experiments and SEM results, the macroscopic mechanical and microscopic physical properties of gritstone can be explained. The uneven thermal expansion state of various minerals under the action of temperature appears due to the different thermal expansion coefficient of various mineral components in the rocks. The thermal stress is generated between mineral crystal particles, then cracks are initiated if the thermal stress is larger than the yield limit of mineral when the sandstone specimens are subjected to thermal treatments. Furthermore, mineral composition began to decompose and mineral content decreased due to the action of the hydro-thermal action, which accelerate the growth of crack length and width. Finally, the cracks caused by hydro-thermal action would lead to the intergranular fracture in the mineral particles as long as the temperature of hydro-thermal action are large enough. In authors' opinion, the differences in mechanical properties of the gritstone specimen are mainly caused by these microscopic cracks with different characteristics.

CONCLUSION

Many tests show that the physical and mechanical performances of rocks after the serials HTHP treatments are different. In this work, the mechanical properties of the gritstone specimens under the HTHP treatment in laboratory tests are investigated and analyzed, especially the different cooling down effect are also taken into account to fully understand the performance of rocks under the hydrothermal environment.

High temperature and high pressure 150°C hydro-thermal treatment have an obvious effect on the densification stage, elasticity and failure procedures of gritstone. The densification stage prolongs and the rate of slope decreases with the rise of water pressure. Meanwhile, the strength and Young's modulus of specimens in Ht group decrease with increasing water pressure. While, the cooling down treatment has a great effect on the densification stage, elasticity and failure procedures of specimens in Cd group with no obvious pattern.

In the Ht group, the STS^S of specimens are decreasing with the increase of water pressure. Meantime, the peak displacement is increasing with the increase of water pressure. In the Cd group, the STS^S and peak displacement of specimen WP1 are the lowest one. While, the STS^S of specimen W1 is the biggest one. The differences in mechanical properties of the gritstone specimen are mainly caused by the ablation effect in the microscale under different HTHP and cooling down conditions.

The surface deformation characteristics of the tested gritstone specimens are investigated by analyzing the full strain field and the local strain concentration. In the gritstone specimen, the major principal strain is first concentrated in the bottom or the top of gritstone specimens where the crack is initiated. The small jump of local strain means crack initiation and propagation, while the fracture of strain gauge leads to strain mutation.

DATA AVAILABILITY STATEMENT

The datasets generated for this study are available on request to the corresponding author.

AUTHOR CONTRIBUTIONS

YZ proposed the topic. JB was in charge of experiments and wrote most of the manuscript. XZ and YH were in charge of part of experiments and revised manuscript.

FUNDING

This work was supported by the Natural Science Foundation Project of CQ CSTC (No. cstc2017jcyjA1250), Talents of Guizhou University (Grant No. 201901), the Special Research Funds of Guizhou University (Grant No. 201903), and Guizhou joint support project ([2018]2787).

REFERENCES

AbuAisha, M., Loret, B., and Eaton, D. (2016). Enhanced geothermal systems (EGS): hydraulic fracturing in a thermo-poroelastic framework. *J. Petrol. Sci. Eng.* 146, 1179–1191.

Bahaaddini, M., Serati, M., Masoumi, H., and Rahimi, E. (2019). Numerical assessment of rupture mechanisms in Brazilian test of brittle materials. *Int. J. Sol. Struct.* 181, 1–12. doi: 10.1016/j.ijsolstr.2019.07.004

Bi, J., and Zhou, X. P. (2015). Numerical simulation of zonal disintegration of the surrounding rock masses around a deep circular tunnel under dynamic unloading. *Int. J. Comp. Meth. Sing* 12:15500203.

Bi, J., and Zhou, X. P. (2017a). A novel numerical algorithm for simulation of initiation, propagation and coalescence of flaws subject to internal fluid pressure and vertical stress in the framework of general particle dynamics. *Rock Mech. Rock Eng.* 50, 1–17.

Bi, J., and Zhou, X. P. (2017b). Numerical simulation of kinetic friction in the fracture process of rocks in the framework of general particle dynamics. *Comput. Geotech.* 83, 1–15. doi: 10.1016/j.compgeo.2016.10.019

Bi, J., Zhou, X. P., and Qian, Q. H. (2016a). The 3D numerical simulation for the propagation process of multiple pre-existing flaws in rock-like materials subjected to biaxial compressive loads. *Rock Mech. Rock Eng.* 49, 1611–1627. doi: 10.1007/s00603-015-0867-y

Bi, J., Zhou, X. P., and Xu, X. M. (2016b). Numerical simulation of failure process of rock-like materials subjected to impact loads. *Int. J. Geomech.* 17:04016073. doi: 10.1061/(asce)gm.1943-5622.0000769

Bonte, M., Stuyfzand, P. J., and Breukelen, B. M. V. (2014). Reactive transport modeling of thermal column experiments to investigate the impacts of aquifer thermal energy storage on groundwater quality. *Environ. Sci. Technol.* 48, 12099–12107. doi: 10.1021/es502477m

Breede, K., Dzebisashvili, K., Liu, X., and Falcone, G. (2013). A systematic review of enhanced (or engineered) geothermal systems: past, present and future. *Geotherm. Energ.* 1:4.

Chen, Y., Ma, G., and Wang, H. (2018). The simulation of thermo-hydro-chemical coupled heat extraction process in fractured geothermal reservoir. *Appl. Therm. Eng.* 143, 859–870. doi: 10.1016/j.applthermaleng.2018.08.015

Dutt, A., Saini, M. S., Singh, T. N., Verma, A. K., and Bajpai, R. K. (2012). Analysis of thermo-hydrologic-mechanical impact of repository for high-level radioactive waste in clay host formation: an Indian reference disposal system. *Environ. Earth Sci.* 66, 2327–2341. doi: 10.1007/s12665-011-1455-4

El Sharawy, M. S., and Nabawy, B. S. (2019). Integration of electrofacies and hydraulic flow units to delineate reservoir quality in uncored reservoirs: a case study, Nubia Sandstone Reservoir, Gulf of Suez, Egypt. *Nat. Resour. Res.* 28, 1587–1608. doi: 10.1007/s11053-018-9447-7

Gautam, P. K., Verma, A. K., Maheshwar, S., and Singh, T. N. (2016). Thermomechanical analysis of different types of sandstone at elevated temperature. *Rock Mech. Rock Eng.* 49, 1985–1993. doi: 10.1007/s00603-015-0797-8

Griffioen, J., and Appelo, C. A. J. (1993). Nature and extent of carbonate precipitation during aquifer thermal energy storage. *Appl. Geochem.* 8, 161–176. doi: 10.1016/0883-2927(93)90032-c

Gruber, C., Kutuzov, I., and Ganor, J. (2016). The combined effect of temperature and pH on albite dissolution rate under far-from-equilibrium conditions. *Geochim. Cosmochim. Ac* 186, 154–167. doi: 10.1016/j.gca.2016.04.046

Guha Roy, D., and Singh, T. N. (2016). Effect of heat treatment and layer orientation on the tensile strength of a crystalline rock under brazilian test condition. *Rock Mech. Rock Eng.* 49, 1663–1677. doi: 10.1007/s00603-015-0891-y

Holmslykke, H. D., Kjøller, C., and Fabricius, I. L. (2017). Core flooding experiments and reactive transport modeling of seasonal heat storage in the hot deep gassum sandstone formation. *ACS Earth Space Chem.* 1, 251–260. doi: 10.1021/acsearthspacechem.7b00031

Hudson, J. A., Bäckström, A., Rutqvist, J., Lanru, J., Tobias, B., Masakazu, C., et al. (2009). Characterising and modelling the excavation damaged zone in crystalline rock in the context of radioactive waste disposal. *Environ. Geol.* 57, 1275–1297. doi: 10.1007/s00254-008-1554-z

Isrm (1978). Suggested methods for determining tensile strength of rock materials. *Int. J. Rock Mech. Min.* 15, 99–103. doi: 10.1016/0148-9062(78)90003-7

Kumari, W. G. P., Ranjith, P. G., Perera, M. S. A., Li, X., Li, L. H., Chen, B. K., et al. (2018). Hydraulic fracturing under high temperature and pressure conditions with micro CT applications: geothermal energy from hot dry rocks. *Fuel* 230, 138–154. doi: 10.1016/j.fuel.2018.05.040

Lund, J. W., Freeston, D. H., and Boyd, T. L. (2011). Direct utilization of geothermal energy 2010 worldwide review. *Geothermics* 40, 159–180. doi: 10.1016/j.geothermics.2011.07.004

Ngwenya, B. T., Elphick, S. C., Main, I. G., and Shimmield, G. B. (2000). Experimental constraints on the diagenetic self-sealing capacity of faults in high porosity rocks. *Earth Planet. Sci. Lett.* 183, 187–199. doi: 10.1016/s0012-821x(00)00261-2

Pandey, S. N., Chaudhuri, A., Kelkar, S., Sandeep, V. R., and Rajaram, H. (2014). Investigation of permeability alteration of fractured limestone reservoir due to geothermal heat extraction using three-dimensional thermo-hydro-chemical (THC) model. *Geothermics* 51, 46–62. doi: 10.1016/j.geothermics.2013.11.004

Pandey, S. N., Vishal, V., and Chaudhuri, A. (2018). Geothermal reservoir modeling in a coupled thermo-hydro-mechanical-chemical approach: a review. *Earth Sci. Rev.* 185, 1157–1169. doi: 10.1016/j.earscirev.2018.09.004

Possemiers, M., Huysmans, M., and Batelaan, O. (2014). Influence of aquifer thermal energy storage on groundwater quality: a review illustrated by seven case studies from Belgium. *J. Hydrol. Reg. Stud.* 2, 20–34. doi: 10.1016/j.ejrh.2014.08.001

Rawal, C., and Ghassemi, A. (2014). A reactive thermo-poroelastic analysis of water injection into an enhanced geothermal reservoir. *Geothermics* 50, 10–23. doi: 10.1016/j.geothermics.2013.05.007

Réveillère, A., Hamm, V., Lesueur, H., Cordier, E., and Goblet, P. (2013). Geothermal contribution to the energy mix of a heating network when using aquifer thermal energy storage: modeling and application to the Paris basin. *Geothermics* 47, 69–79. doi: 10.1016/j.geothermics.2013.02.005

Schmidt, R. B., Bucher, K., Drüppel, K., and Stober, I. (2017). Experimental interaction of hydrothermal Na-Cl solution with fracture surfaces of geothermal reservoir sandstone of the upper rhine graben. *Appl. Geochem.* 81, 36–52. doi: 10.1016/j.apgeochem.2017.03.010

Sengun, N. (2014). Influence of thermal damage on the physical and mechanical properties of carbonate rocks. *Arab. J. Geosc.* 7, 5543–5551. doi: 10.1007/s12517-013-1177-x

Shi, Y., Song, X., Li, G., Li, R., Zhang, Y., Wang, Y., et al. (2018). Numerical investigation on heat extraction performance of a downhole heat exchanger geothermal system. *Appl. Therm. Eng.* 134, 513–526. doi: 10.1016/j.applthermaleng.2018.02.002

Singh, B., Ranjith, P. G., Chandrasekharam, D., Viete, D., Singh, H. K., Lashin, A., et al. (2015). Thermo-mechanical properties of bundelkhand granite near Jhansi, India. *Geomech. Geophy. Geo-Energy and Geo Res.* 1, 35–53. doi: 10.1007/s40948-015-0005-z

Sirdesai, N. N., Singh, T. N., Ranjith, P. G., and Singh, R. (2017). effect of varied durations of thermal treatment on the tensile strength of Red Sandstone. *Rock Mech. Rock Eng.* 50, 205–213. doi: 10.1007/s00603-016-1047-4

Ulusay, R. (2014). The Isrm suggested methods for rock characterization, testing and monitoring: 2007-2014. *Springer Intern. Publish.* 15, 47–48.

Vetter, A., Mangelsdorf, K., Schettler, G., Seibt, A., Wolfgramm, M., Rauppach, K., et al. (2012). Fluid chemistry and impact of different operating modes on microbial community at Neubrandenburg heat storage (Northeast German Basin). *Org. Geochem.* 53, 8–15. doi: 10.1016/j.orggeochem.2012.08.008

Wang, F., and Konietzky, H. (2019). Thermo-Mechanical properties of granite at elevated temperatures and numerical simulation of thermal cracking. *Rock Mech. Rock Eng.* 52, 3737–3755. doi: 10.1007/s00603-019-01837-1

Yang, S., Huang, Y., Tian, W., Yin, P., and Jing, H. (2019). Effect of high temperature on deformation failure behavior of granite specimen containing a single fissure under uniaxial compression. *Rock Mech. Rock Eng.* 52, 2087–2107. doi: 10.1007/s00603-018-1725-5

Yao, W., Xu, Y., Wang, W., and Kanopolous, P. (2016). Dependence of dynamic tensile strength of longyou sandstone on heat-treatment temperature and loading rate. *Rock Mech. Rock Eng.* 49, 3899–3915. doi: 10.1007/s00603-015-0895-7

Zhang, F., Jiang, P., and Xu, R. (2013). System thermodynamic performance comparison of CO2-EGS and water-EGS systems. *Appl. Therm. Eng.* 61, 236–244. doi: 10.1016/j.applthermaleng.2013.08.007

Zhao, Y., He, P., Zhang, Y., and Wang, C. (2018a). A new criterion for a toughness-dominated hydraulic fracture crossing a natural frictional interface. *Rock Mech. Rock Eng.* 52, 2617–2629.

Zhao, Y., Zhang, L., Wang, W., Wan, W., and Ma, W. (2018b). Separation of elastoviscoplastic strains of rock and a nonlinear creep model. *Int. J. Geomech.* 18:040171291.

Zhao, Y., Wang, Y., Wang, W., Tang, L., Liu, Q., and Cheng, C. (2019). Modeling of rheological fracture behavior of rock cracks subjected to hydraulic pressure and far field stresses. *Theor. Appl. Fract. Mec.* 101, 59–66. doi: 10.1016/j.tafmec.2019.01.026

Zhao, Y., Wang, Y., Wang, W., Wan, W., and Tang, J. (2017a). Modeling of non-linear rheological behavior of hard rock using triaxial rheological experiment. *Int. J. Rock Mech. Min.* 93, 66–75. doi: 10.1016/j.ijrmms.2017.01.004

Zhao, Y., Zhang, L., Wang, W., Tang, J., Lin, H., and Wan, W. (2017b). Transient pulse test and morphological analysis of single rock fractures. *Int. J. Rock Mech. Min.* 91, 139–154. doi: 10.1016/j.ijrmms.2016.11.016

Zhao, Y., Zhang, L., Wang, W., Pu, C., Wan, W., and Yang, J. (2016). Cracking and stress–strain behavior of rock-like material containing two flaws under uniaxial compression. *Rock Mech. Rock Eng.* 49, 2665–2687. doi: 10.1007/s00603-016-0932-1

Zhou, X., Bi, J., Deng, R., and Li, B. (in press). Effects of brittleness on crack behaviors in rock-like materials. *J. Test Eval.* 48. doi: 10.1520/JTE20170595

Zhou, X. P., and Bi, J. (2016). 3D numerical study on the growth and coalescence of pre-existing flaws in rocklike materials subjected to uniaxial compression. *Int. J. Geomech.* 16:04015096. doi: 10.1061/(asce)gm.1943-5622.0000565

Zhou, X. P., and Bi, J. (2018). Numerical simulation of thermal cracking in rocks based on general particle dynamics. *J. Eng. Mech.* 144:040171561.

Zhu, T., and Huang, D. (2019). Experimental investigation of the shear mechanical behavior of sandstone under unloading normal stress. *Int. J. Rock Mech. Min.* 114, 186–194. doi: 10.1016/j.ijrmms.2019.01.003

Conflict of Interest: The authors declare that the research was conducted in the absence of any commercial or financial relationships that could be construed as a potential conflict of interest.